

Strain engineering of topological magnons in chromium trihalides from first-principles

Dorye L. Esteras and José J. Baldoví*
*Instituto de Ciencia Molecular, Universitat de València,
Catedrático José Beltrán 2, 46980 Paterna, Spain.*

Recent experiments evidence the direct observation of spin waves in chromium trihalides and a gap at the Dirac points of the magnon dispersion in bulk CrI_3 . However, the topological origin of this feature remains unclear and its emergence at the 2D limit has not yet been proven experimentally. Herein, we perform a fully self-consistent ab initio analysis that supports the presence of topological magnons in chromium trihalides monolayers. Our results confirm the existence of a gap around the K high-symmetry point in the linear magnon dispersion of CrI_3 , which originates as a direct consequence of intralayer Dzyaloshinskii-Moriya (DM) interaction. In addition, our orbital resolved analysis reveals the microscopic mechanisms that can be exploited using strain engineering to increase the strength of the DM interaction and thus control the gap size in CrI_3 . This paves the way to the further development of this family of materials as building-blocks for topological magnonics at the limit of miniaturization.

I. INTRODUCTION

Two-dimensional (2D) materials have become a focus of intense research due to their unique physical and chemical properties [1–3]. The recent discovery of long-range magnetic order in 2D van der Waals layered materials down to the single layer has opened new frontiers for the exploration of 2D magnetism and the development of novel spin-based applications at the nanoscale [4, 5]. A stimulating challenge in this direction is the control of collective spin excitations, also known as spin waves –and their quanta magnons–, which are present in magnetically ordered materials [6–10]. Magnons can be used to store, process and transmit information, and thus open the door to low-energy consumption nanodevices with higher tunability, excellent integrability and many other advantages pursued by the emergent field of magnonics [11–14]. Furthermore, recent research has led to new insights into the topology of these collective magnetic excitations, indicating that non-trivial topological phases of matter can arise within magnon band structures [15–18]. This offers a promising platform to drive topological transitions using magnetic fields and generate topologically protected spin currents. Another well-known advantage of 2D materials is the possibility of tuning their properties via mechanical strain, which has been culminated in the field of straintronics [19–22]. In the context of 2D magnetic materials, strain engineering has allowed the enhancement of the magnetic anisotropy energy and spin-spin interactions of chromium trihalides (CrX_3 , $X = \text{Cl, Br, I}$) [23–26], and has been recently extended to the realm of magnonics in CrSBr [27].

Ferromagnetic (FM) honeycomb lattices provide ideal building-blocks to search for topological magnon excitations. The symmetry of these systems creates linear

Dirac dispersions in the magnon band structure around the K high-symmetry point, where time-reversal symmetry is broken [28, 29]. Consequently, the CrX_3 family stays in the line of fire [30–33] since the experimental observation of spin waves in all three compounds has been reported [16–18, 34, 35]. Moreover, the last empirical evidence points towards the topological nature of these magnons, suggesting that this class of 2D materials can be useful for topological magnonic applications [36–40]. The non-trivial topology arises from gapped Dirac cones in the magnon dispersion, but depends crucially on the origin of this gap, which has been experimentally measured in bulk CrI_3 [16, 41]. However, the mechanism behind this feature still remains controversial [42–46] and the survival of the topological gap at the 2D limit is unexplored. Indeed, the possibility of carrying out inelastic neutron scattering measurements in monolayer chromium trihalides represents a gigantic challenge, which imposes an important restriction to understand the origin of the gap in the absence of interlayer magnetic exchange interactions.

To unveil the microscopic origin of topologically protected magnons in 2D chromium trihalides, herein, we perform a fully self-consistent Hubbard-corrected ab initio investigation of CrCl_3 , CrBr_3 and CrI_3 followed by a derived Wannier-based tight-binding model. Our optimized self-consistent parameter-free workflow predicts the presence of a clear topological gap in CrI_3 and a very small gap of CrBr_3 in the absence of interlayer interactions, revealing important details about the underlying mechanisms behind its formation. In particular, we illustrate the crucial role of Dzyaloshinskii-Moriya (DM) interactions and rationalize it by means of an orbital-resolved magnetic exchange analysis. Then, we apply biaxial strain engineering in order to enhance DM interaction, which results in the possibility of observing a drastic increase of the topological gap in CrI_3 . Our results pave the way for the use of 2D chromium trihalides as building components for topological magnonic devices.

* j.jaime.baldovi@uv.es

II. RESULTS AND DISCUSSION

At low temperature, chromium trihalide monolayers have a trigonal structure with point group symmetry D_{3d} . The Cr atoms form a honeycomb lattice with long-range FM order where each Cr ($S = 3/2$) is surrounded by an octahedral environment, coordinated by an edge-sharing octahedra formed by six halide atoms. A sizeable magneto-crystalline anisotropy originated by the spin-orbit coupling (SOC) of the ligands, stabilizes the spin off-plane, with the exception of CrCl_3 where the combination of the weak SOC from the Cl atoms and the magnetic dipolar anisotropy energy results in an in-plane ferromagnetic order [47–49]. Fig. 1 presents the crystal structure of CrX_3 and a scheme of the main magnetic exchange interactions between the Cr^{3+} ions, where the interaction between first neighbours, namely J_1 , takes place through the ligands in a cation-anion-cation super-exchange interaction. Second (J_2) and third (J_3) order interactions can be explained according to more complex cation-anion-anion-cation pathways. The arrangement of ligands across the honeycomb structure provides a set of Cr-X-Cr and Cr-X-X-Cr angles of close to 90° for J_1 , J_2 and to 130° in the case of J_3 that agrees with the expected FM/AFM behaviour described by the Goodenough-Kanamori-Anderson (GKA) rules. Despite these findings, the microscopic explanation behind the exchange mechanisms has proven to correspond to a more complex picture originated by FM/AFM competitions between t_{2g} - e_g and t_{2g} - t_{2g} spin channels that results in the previous mentioned FM J_1 , J_2 and AFM J_3 [50–53].

To describe the electronic properties of CrX_3 , we perform fully self-consistent Hubbard-corrected density functional theory (DFT + U) calculations [54, 55]. The Hubbard U parameter is computed by means of linear response through density functional perturbation theory and this process is repeated in several optimization cycles until convergence of both U and crystal structure are achieved. As a result of this fully free-parameter DFT+U approach, we find that the converged Hubbard U increases as soon as we move down in the periodic table from Cl to I. In particular, the U values for CrCl_3 , CrBr_3 and CrI_3 are 3.96, 4.20 and 4.55 eV, respectively. This evolution naturally follows the expected behaviour of Hubbard U under ligand variation, where the occupations of hybridized transition metals experiment the effect of environment, that enhances the energy to add/remove electrons according to the electronegativity of the ligands ($\text{I} > \text{Br} > \text{Cl}$) [56].

Then, we compute the electronic band structure of CrCl_3 , CrBr_3 and CrI_3 for their respective fully optimized structures (Fig. S??). In the octahedral environment of Cr^{3+} , the d levels split into a lower energy t_{2g} triplet and a higher energy e_g doublet, where the three electrons of the magnetic atom occupy the t_{2g} manifold. The calculated electronic structures show band gaps between these two manifolds of 2.00, 1.35 and 0.75 eV for CrCl_3 , CrBr_3 and CrI_3 , respectively.

This decrease from Cl to I indicates the insufficiency of a purely ionic description to characterize the electronic structure of CrX_3 . The role of the ligand requires to be explained with a more quantitative molecular picture, where the electronic structure is influenced by the hybridization of the ligands, depending on their character, atomic weight and structure [57, 58]. The orbital resolved density of states, reported in Fig. S??, shows the most relevant contributing orbitals around the Fermi level. These are mainly d orbitals of Cr and p orbitals of the halide. One can observe that around the Fermi energy the contribution of p orbitals of the halides is extremely important. This indicates a high level of hybridization with the d orbitals of Cr. In opposition, the higher energies in the conduction bands are mainly originated by the empty spin-down t_{2g} d orbitals of Cr. Furthermore, the more external p orbitals in I atoms are weakly bounded to the nucleus resulting in higher energy bands, where in contrast hybridization with Cl atoms arises deeper in energies along the bands. This higher energy hybridization originated by the p orbitals at the edges of valence band, result in a narrower band gap in CrI_3 .

To analyze the magnetic properties of chromium trihalides, we follow an efficient workflow [27] based on purely self-consistent first-principles DFT+U simulations followed by a derived Wannier tight-binding model [59]. This allows to obtain the magnetic exchange interactions (eq. (1)) in an effective Heisenberg spin Hamiltonian, which is evaluated using the Green’s function method as implemented in the TB2J software [60], without any free parameter. Eq. (1) presents the spin Hamiltonian, which includes isotropic, symmetric anisotropic and Dzyaloshinskii–Moriya (DM) interactions, as well as a last term considering the single ion anisotropy. This output is then used to obtain the orbital contribution to magnetic exchange, Curie temperature and magnon dispersion (See Computational Methods). This methodology avoids the calculation of exchange interactions using the brute force energy method, and presents a very efficient and easy to automatize route to study magnons in 2D materials. In the case of the CrX_3 family, the reduced basis set is formed by the d orbitals of Cr and the p orbitals of the halide, owing to their major role in stabilizing long-range magnetic order in these materials.

$$H = - \sum_{i \neq j} J_{ij} \vec{S}_i \cdot \vec{S}_j - \sum_{i \neq j} \vec{D}_{ij} \left(\vec{S}_i \times \vec{S}_j \right) - \sum_i A(\vec{S}_i^z)^2 \quad (1)$$

To provide a microscopic understanding of the magnetic properties, we perform an orbital resolved decomposition of the magnetic exchange interactions. Within this approach, we unveil the contributions of the different orbitals to the magnetic exchange channels and magneto-structural correlations in this class of materials (Fig. S??-S??). As observed in previous works, the most important magnetic exchange interactions correspond to the first neighbour (J_1) which are dominated by both

$t_{2g}-t_{2g}$ (AFM) and $t_{2g}-e_g$ (FM) orbital channels. Hence, global exchange interactions are originated from the competition between the AFM and FM mechanisms, where the ligands play an important role in the intensity of the exchange interactions. This is illustrated in Fig. 1, which shows the main interaction channels of CrX_3 represented by the Wannier functions of Cr atoms and ligands. A more detailed analysis of the orbital resolved exchange pathways in these three materials can be found in Fig. S??-S??.

Subsequently, we evaluate the computed spin Hamiltonian parameters under applied biaxial strain (see Fig. 2). For that we distort the in-plane lattice vectors in a range of $\pm 5\%$ and scan different values of the Hubbard U in a range of 2 - 6 eV. The exchange parameters are condensed in effective equations of the form indicated by eq. (2) using the least squares method, which are used then to create a dense dataset.

$$J = \sum_{i=1}^2 \sum_{j=1}^2 = a_{ij} U^i \epsilon^j \quad (2)$$

Fig. 2 presents the evolution of exchange interactions for CrX_3 where a global enhancement can be observed in all the interactions as long as the Hubbard U is increased. In opposition, the effect of strain is different between J_2 and the other interactions. In particular, tensile strain produces a clear enhancement, while in J_2 , compression is required to increase the intensity of the exchange parameters. This complex behaviour can be successfully understood in terms of the orbital resolved analysis presented in Fig. S??-S??. According to Fig. S??, Fig. S?? and Fig. S??, the application of tensile strain to the lattice reduces AFM interactions, thus resulting in a more FM system. The increase of the Hubbard U also supports this enhanced FM character increasing the $t_{2g}-e_g$ channel. In the particular case of CrI_3 , an additional element plays a role, the AFM contribution via $d_{z2}-d_{z2}$ and $d_{x2y2}-d_{x2y2}$ becomes relevant and compete with the FM pathway $d_{z2}-d_{x2y2}$, cancelling each other (Fig. S??). As long as the material is elongated, these AFM channels become less important, generating a new source of FM contribution characteristic of CrI_3 . The increase of Hubbard U enhances globally the different channels that cancel each other, which results in a less important modification of the exchange interactions that can be observed in Fig. 2, where the evolution of J_1 respect to U in CrI_3 can be seen as an increment with a very small slope.

The derived effective equations are used to compute the Curie temperature by solving the quantum Heisenberg model up to third nearest neighbours (see Methods). Using the self-consistent Hubbard U for each material and in absence of strain, we obtain Curie temperature values of 23.0, 55.3 and 94.2 K for CrCl_3 , CrBr_3 and CrI_3 , respectively, which overestimate the experimental temperatures of 13.0, 34.0 and 45.0 K [4, 61, 62]. Nevertheless, they are in good agreement with state-of-the-art calculations based on first principles methods [63, 64].

Fig. 3 represents the T_C evolution in terms of strain and Hubbard U for each CrX_3 . As one may observe the trends are very similar in the case of CrCl_3 and CrBr_3 , although differences in the amplitude of exchange parameters produce a different derivative of Curie temperature in the maps. On the other hand, CrI_3 gives a slightly different trend, which can be rationalized in terms of the dissimilar behaviour of exchange channels (Fig. 2) and the presence of e_g-e_g interactions, which are characteristic of this material. Regarding the impact of strain on T_C , our calculations evidence that T_C is expected to increase in the three derivatives via stretching up to a 50, 30, 15% in CrCl_3 , CrBr_3 and CrI_3 , respectively. In addition, we can observe that when CrCl_3 and CrI_3 are compressed below $\sim 3\%$, the maps have regions coloured in white, in which the anisotropy becomes very weak. In these conditions the magnetic anisotropy energy is expected to be fully dominated by shape anisotropy, favouring the in-plane orientation of spins.

Afterwards, we calculate the magnon dispersion for each 2D ferromagnet, considering the spin Hamiltonian in eq. (1) (see methods). In Fig. 4 we can visualize the magnon dispersions of CrX_3 , both in equilibrium and under extreme strain conditions ($\pm 5\%$). For all three chromium trihalides, we obtain an overestimation of the magnon energies respect to the inelastic scattering experiments in the bulk using their optimized single-layer structures, however these findings are in agreement with previous reported calculations [65, 66]. We also simulate the magnon dispersion in the absence of DM interaction (Fig. S??) which shows the typical crossing between acoustic and optical modes forming gapless Dirac cones in the K high-symmetry point of the Brillouin zone in all three compounds. The inclusion of the DM interactions opens a gap Δ_k (1.26 meV) in CrI_3 , which is agreement with the values obtained for the bulk in a recently reported DFT study [65, 67]. This opening, results to be purely originated by the DM_{z2} interaction, is absent in CrCl_3 and existent but very small in CrBr_3 (0.26 meV) due to the small DM interactions arising from the SOC.

To elucidate the microscopic origin of the DM-driven topological gap, we performed an orbital resolved analysis of DM interactions. It reveals that, in absence of external strain, the symmetry-allowed z component of DM interaction, and thus the topological gap, arise directly (82%) from the e_g-e_g channels of interaction, where the interaction via $d_{x2-y2}-d_{z2}$ orbital mechanism results to be dominant. The other (18%) is due to the competition between different $t_{2g}-e_g$ orbitals (Fig. S??), being the d_{x2-y2} and d_{xz}/d_{yz} orbitals the most relevant magnetic exchange pathway. These $t_{2g}-e_g$ interactions, tend to cancel each other, given the anisotropic and antisymmetric nature of these interactions.

In order to analyse the effect of strain in the magnon dispersions we determine the Hubbard U self-consistently for each particular strained structure. Fig. S?? illustrates the evolution of Hubbard U under biaxial strain. One can observe that on-site Coulomb repulsion is very

sensitive to the compression/elongation of CrX_3 , giving changes of around 0.5 eV as a function of strain. Then, we simulate the magnon dispersion for the different distorted structures taking into account their corresponding Hubbard U. The magnon dispersion of each material is presented in Fig. 4, where one can see that the effect of strain produces an important modulation of the magnon modes [68], (around $\sim 25\%$ in M high-symmetry point and $\sim 50\%$ of the maximum frequency) increasing the dispersive behaviour between Γ and K in the case of tensile strain. Furthermore, we find that compressive strain tends to shatter the linear energy dispersion relationship around Dirac cone in K high-symmetry point. Regarding the DM_{2z} interaction evolution under strain, we can observe a drastic enhancement by applying tensile biaxial strain in CrI_3 (almost doubled at 5%) as indicated in Fig. 4. This is because the $t_{2g}-e_g$ channels are favoured at the same time that e_g-e_g interactions remain constant. As a result, $t_{2g}-e_g$ interactions become 40% of the contribution to DM interaction resulting in the increase of the topological gap. These results contrast with the ones for CrCl_3 and CrBr_3 where significant changes are not observed (Fig. S??). A possibility to induce a gap opening at the Dirac points of CrBr_3 and CrCl_3 could be the creation of heterostructures with high SOC materials by proximity effects. This could even be exploited in CrCl_3 by achieving a switching between in-plane (Dirac dispersion) and out-of-plane (opened gap) states due to spin-orbit torque effects [69–71].

III. CONCLUSIONS

We performed a fully self-consistent first principles analysis of 2D transition metal trihalides motivated by recent findings that suggest the presence of a topological gap in the magnon spectra of bulk CrI_3 . Our results confirm the existence of a Δ_k gap opening the Dirac cones of CrI_3 down to the 2D limit and discard its presence in CrCl_3 and CrBr_3 . The Δ_k gap emerges as a direct consequence of DM_{2z} interaction, which supports the presence of topological magnons in 2D CrI_3 . This points to a competition between DM interaction and interlayer exchange in the bulk, which is rationalized by means of orbital-resolved magnetic exchange calculations. In particular, our microscopic analysis reveals that the $d_{x^2-y^2}-d_{z^2}$ orbital mechanism is the source of the DM interaction. We applied biaxial strain to exploit the $t_{2g}-e_g$ exchange pathways and increase the robustness of DM interaction, resulting in an increment of the Δ_k gap. This work illus-

trates the possibility of tuning topological magnons by strain engineering of DM interaction.

IV. COMPUTATIONAL METHODS

DFT + U calculations were carried out using the Quantum ESPRESSO package [72]. The generalized gradient approximation (GGA) and the PBE functional were used to describe the exchange correlation energy [73]. We selected standard solid-state US pseudopotentials from the QuantumEspresso database. The electronic wave functions were expanded with well-converged kinetic energy cut-offs for the wave functions and charge density. All the structures were fully optimized using the BFGS algorithm [74] until the forces on each atom were smaller than 1×10^{-3} Ry/au, and the energy difference between two consecutive relaxation steps was less than 1×10^{-4} Ry. The Brillouin zone was sampled by a fine $8 \times 8 \times 1$ Γ -centered k-point Monkhorst-Pack mesh for all calculations [75]. The self consistent Hubbard U and structure were computed until a convergence of 0.01 eV was reached in the Hubbard U. Our DFT + U calculations were followed by Wannier functions calculations using the software Wannier90 [59]. The d orbitals of Cr and the p orbitals of the ligands, were selected as orbital projectors to maximally localize the Wannier functions. Wannier90 calculations were performed ensuring a correct fit to the electronic band structure and spreads. The orbital resolved analysis was performed after rotating the coordinate system of the crystal to align the metal-ligand bonds direction of the octahedra with the cartesian axes. The quantum Heisenberg model was solved to calculate Curie temperature [76] and magnon dispersions were derived using the linear spin wave theory [77], combining positive and negative solutions according to Colpa method [78].

V. ACKNOWLEDGEMENTS

The authors acknowledge the financial support from the European Union (ERC-2021-StG-101042680 2D-SMARTiES and FET-OPEN SINFONIA 964396), the Spanish MICINN (2D-HETEROS PID2020-117152RB-100, cofinanced by FEDER, and Excellence Unit “María de Maeztu” CEX2019-000919-M), and the Generalitat Valenciana (grant CDEIGENT/2019/022 and CIDEIGENT/2018/004). The computations were performed on the Tirant III cluster of the Servei d’Informàtica of the University of Valencia.

[1] Ethan C Ahn. 2d materials for spintronic devices. *npj 2D Materials and Applications*, 4(1):17, 2020.

[2] Tingxin Li, Shengwei Jiang, Nikhil Sivadas, Zefang Wang, Yang Xu, Daniel Weber, Joshua E Goldberger, Kenji Watanabe, Takashi Taniguchi, Craig J Fennie,

- et al. Pressure-controlled interlayer magnetism in atomically thin CrI_3 . *Nature materials*, 18(12):1303–1308, 2019.
- [3] Santosh K Tiwari, Sumanta Sahoo, Nannan Wang, and Andrzej Huczko. Graphene research and their outputs: Status and prospect. *Journal of Science: Advanced Materials and Devices*, 5(1):10–29, 2020.
 - [4] Bevin Huang, Genevieve Clark, Efrén Navarro-Moratalla, Dahlia R Klein, Ran Cheng, Kyle L Seyler, Ding Zhong, Emma Schmidgall, Michael A McGuire, David H Cobden, et al. Layer-dependent ferromagnetism in a van der waals crystal down to the monolayer limit. *Nature*, 546(7657):270–273, 2017.
 - [5] Jae-Ung Lee, Sungmin Lee, Ji Hoon Ryoo, Soonmin Kang, Tae Yun Kim, Pilkwang Kim, Cheol-Hwan Park, Je-Geun Park, and Hyeonsik Cheong. Ising-type magnetic ordering in atomically thin FePS_3 . *Nano letters*, 16(12):7433–7438, 2016.
 - [6] Sergej O Demokritov and Andrei N Slavin. *Magnonics: From fundamentals to applications*, volume 125. Springer Science & Business Media, 2012.
 - [7] Benjamin Lenk, Henning Ulrichs, Fabian Garbs, and Markus Münzenberg. The building blocks of magnonics. *Physics Reports*, 507(4-5):107–136, 2011.
 - [8] VV Kruglyak, SO Demokritov, and D Grundler. Magnonics. *Journal of Physics D: Applied Physics*, 43(26):264001, 2010.
 - [9] Sebastian Neusser and Dirk Grundler. Magnonics: Spin waves on the nanoscale. *Advanced materials*, 21(28):2927–2932, 2009.
 - [10] Anjan Barman, Gianluca Gubbiotti, Sam Ladak, Adekunle Olusola Adeyeye, Maciej Krawczyk, Joachim Gräfe, Christoph Adelman, Sorin Cotofana, Azad Naeemi, Vitaliy I Vasyuchka, et al. The 2021 magnonics roadmap. *Journal of Physics: Condensed Matter*, 33(41):413001, 2021.
 - [11] Andrii V Chumak, Vitaliy I Vasyuchka, Alexander A Serga, and Burkard Hillebrands. Magnon spintronics. *Nature physics*, 11(6):453–461, 2015.
 - [12] Aleksandr Rodin, Maxim Trushin, Alexandra Carvalho, and AH Castro Neto. Collective excitations in 2d materials. *Nature Reviews Physics*, 2(10):524–537, 2020.
 - [13] Sebastian Neusser and Dirk Grundler. Magnonics: Spin waves on the nanoscale. *Advanced materials*, 21(28):2927–2932, 2009.
 - [14] Sergei Apollonovich Nikitov, Dmitry Vladimirovich Kalyabin, Ivan Viktorovich Lisenkov, Andrei Nikolaevich Slavin, Yu N Barabanenkov, Sergey Aleksandrovich Osokin, Alexandr Vladimirovich Sadovnikov, Evgeniy Nikolaevich Beginin, Mariya Aleksandrovna Morozova, Yu P Sharaevsky, et al. Magnonics: a new research area in spintronics and spin wave electronics. *Physics-Uspekhi*, 58(10):1002, 2015.
 - [15] XS Wang and XR Wang. Topological magnonics. *Journal of Applied Physics*, 129(15):151101, 2021.
 - [16] Lebing Chen, Jae-Ho Chung, Matthew B Stone, Alexander I Kolesnikov, Barry Winn, V Ovidiu Garlea, Douglas L Abernathy, Bin Gao, Mathias Augustin, Elton JG Santos, et al. Magnetic field effect on topological spin excitations in CrI_3 . *Physical Review X*, 11(3):031047, 2021.
 - [17] Stanislav E Nikitin, Björn Fåk, Karl W Krämer, Tom Fennell, Bruce Normand, Andreas M Läuchli, and Ch Rüegg. Thermal evolution of dirac magnons in the honeycomb ferromagnet CrBr_3 . *Physical review letters*, 129(12):127201, 2022.
 - [18] Lebing Chen, Matthew B Stone, Alexander I Kolesnikov, Barry Winn, Wonhyuk Shon, Pengcheng Dai, and Jae-Ho Chung. Massless dirac magnons in the two dimensional van der waals honeycomb magnet CrI_3 . *2D Materials*, 9(1):015006, 2021.
 - [19] Kuntal Roy, Supriyo Bandyopadhyay, and Jayasimha Atulasimha. Hybrid spintronics and straintronics: A magnetic technology for ultra low energy computing and signal processing. *Applied Physics Letters*, 99(6):063108, 2011.
 - [20] Anastas Akhmetovich Bukharaev, Anatolii K Zvezdin, Aleksandr P Pyatakov, and Yuri K Fetisov. Straintronics: a new trend in micro-and nanoelectronics and materials science. *Physics-Uspekhi*, 61(12):1175, 2018.
 - [21] Rafael Roldán, Andrés Castellanos-Gomez, Emmanuele Cappelluti, and Francisco Guinea. Strain engineering in semiconducting two-dimensional crystals. *Journal of Physics: Condensed Matter*, 27(31):313201, 2015.
 - [22] Andres Castellanos-Gomez, Rafael Roldán, Emmanuele Cappelluti, Michele Buscema, Francisco Guinea, Herre SJ van der Zant, and Gary A Steele. Local strain engineering in atomically thin MoS_2 . *Nano letters*, 13(11):5361–5366, 2013.
 - [23] Lucas Webster and Jia-An Yan. Strain-tunable magnetic anisotropy in monolayer CrI_3 , CrBr_3 , and CrI_3 . *Physical Review B*, 98(14):144411, 2018.
 - [24] Zewen Wu, Jin Yu, and Shengjun Yuan. Strain-tunable magnetic and electronic properties of monolayer CrI_3 . *Physical Chemistry Chemical Physics*, 21(15):7750–7755, 2019.
 - [25] Tista Mukherjee, Suman Chowdhury, Debnarayan Jana, and LC Lew Yan Voon. Strain induced electronic and magnetic properties of 2d magnet CrI_3 : a dft approach. *Journal of Physics: Condensed Matter*, 31(33):335802, 2019.
 - [26] Sahar Izadi Vishkayi, Zahra Torbatian, Alireza Qaiumzadeh, and Reza Asgari. Strain and electric-field control of spin-spin interactions in monolayer CrI_3 . *Physical Review Materials*, 4(9):094004, 2020.
 - [27] Dorye L Esteras, Andrey Rybakov, Alberto M Ruiz, and José J Baldoví. Magnon straintronics in the 2d van der waals ferromagnet CrBr_3 from first-principles. *Nano Letters*, 22(21):8771–8778, 2022.
 - [28] Sergey S Pershoguba, Saikat Banerjee, JC Lashley, Jihwey Park, Hans Ågren, Gabriel Aeppli, and Alexander V Balatsky. Dirac magnons in honeycomb ferromagnets. *Physical Review X*, 8(1):011010, 2018.
 - [29] Shuyi Li and Andriy H Nevidomskyy. Topological weyl magnons and thermal hall effect in layered honeycomb ferromagnets. *Physical Review B*, 104(10):104419, 2021.
 - [30] António T Costa, Daniel Lourenço R Santos, Nuno MR Peres, and Joaquín Fernández-Rossier. Topological magnons in CrI_3 monolayers: an itinerant fermion description. *2D Materials*, 7(4):045031, 2020.
 - [31] Esteban Aguilera, Rodrigo Jaeschke-Ubiergo, Nicolas Vidal-Silva, Luis EF Foa Torres, and AS Nunez. Topological magnonics in the two-dimensional van der waals magnet CrI_3 . *Physical Review B*, 102(2):024409, 2020.
 - [32] Santu Baidya, Jaejun Yu, and Choong H Kim. Tunable magnetic topological insulating phases in monolayer CrI_3 . *Physical Review B*, 98(15):155148, 2018.
 - [33] M Soenen, C Bacaksiz, RM Menezes, and MV Milosevic. Stacking-dependent topological magnons in bilayer CrI_3 .

- arXiv preprint arXiv:2301.02502*, 2023.
- [34] EJ Samuelsen, Richard Silbergliitt, G Shirane, and JP Remeika. Spin waves in ferromagnetic cr br 3 studied by inelastic neutron scattering. *Physical Review B*, 3(1):157, 1971.
- [35] Zhengwei Cai, Song Bao, Zhao-Long Gu, Yi-Peng Gao, Zhen Ma, Yanyan Shangguan, Wenda Si, Zhao-Yang Dong, Wei Wang, Yizhang Wu, et al. Topological magnon insulator spin excitations in the two-dimensional ferromagnet crbr 3. *Physical Review B*, 104(2):L020402, 2021.
- [36] Joseph Sklenar and Wei Zhang. Self-hybridization and tunable magnon-magnon coupling in van der waals synthetic magnets. *Physical Review Applied*, 15(4):044008, 2021.
- [37] Davit Ghazaryan, Mark T Greenaway, Zihao Wang, Victor H Guarochico-Moreira, Ivan J Vera-Marun, Jun Yin, Yuanxun Liao, Sergey V Morozov, Oleg Kristanovski, Alexander I Lichtenstein, et al. Magnon-assisted tunnelling in van der waals heterostructures based on crbr3. *Nature Electronics*, 1(6):344–349, 2018.
- [38] Maxime Dupont, Yaroslav O Kvashnin, Mahroo Shiranzai, Jonas Fransson, Nicolas Lafforencie, and Adrian Kantian. Monolayer crcl 3 as an ideal test bed for the universality classes of 2d magnetism. *Physical review letters*, 127(3):037204, 2021.
- [39] David MacNeill, Justin T Hou, Dahlia R Klein, Pengxiang Zhang, Pablo Jarillo-Herrero, and Luqiao Liu. Gigahertz frequency antiferromagnetic resonance and strong magnon-magnon coupling in the layered crystal crcl 3. *Physical review letters*, 123(4):047204, 2019.
- [40] Doried Ghader, Heng Gao, Paolo G Radaelli, Alessandra Continenza, and Alessandro Stroppa. Theoretical study of magnon spin currents in chromium trihalide heterobilayers: Implications for magnonic and spintronic devices. *ACS Applied Nano Materials*, 5(10):15150–15161, 2022.
- [41] Lebing Chen, Jae-Ho Chung, Tong Chen, Chunruo Duan, Astrid Schneidewind, Igor Radelytskyi, David J Voneshen, Russell A Ewings, Matthew B Stone, Alexander I Kolesnikov, et al. Magnetic anisotropy in ferromagnetic cri 3. *Physical Review B*, 101(13):134418, 2020.
- [42] Thomas Olsen. Unified treatment of magnons and excitons in monolayer cri 3 from many-body perturbation theory. *Physical Review Letters*, 127(16):166402, 2021.
- [43] Rodrigo Jaeschke-Ubiergo, E Suárez Morell, and Alvaro Sebastian Nunez. Theory of magnetism in the van der waals magnet cri 3. *Physical Review B*, 103(17):174410, 2021.
- [44] Li-Chuan Zhang, Fengfeng Zhu, Dongwook Go, Fabian R Lux, Flaviano José dos Santos, Samir Lounis, Yixi Su, Stefan Blügel, and Yuriy Mokrousov. Interplay of dzyaloshinskii-moriya and kitaev interactions for magnonic properties of heisenberg-kitaev honeycomb ferromagnets. *Physical Review B*, 103(13):134414, 2021.
- [45] Subhadeep Bandyopadhyay, Finn Lasse Buessen, Ritwik Das, Franz G Utermohlen, Nandini Trivedi, Arun Paramekanti, and Indra Dasgupta. Exchange interactions and spin dynamics in the layered honeycomb ferromagnet cri 3. *Physical Review B*, 105(18):184430, 2022.
- [46] Inhee Lee, Franz G Utermohlen, Daniel Weber, Kyusung Hwang, Chi Zhang, Johan van Tol, Joshua E Goldberger, Nandini Trivedi, and P Chris Hammel. Fundamental spin interactions underlying the magnetic anisotropy in the kitaev ferromagnet cri 3. *Physical Review Letters*, 124(1):017201, 2020.
- [47] Feng Xue, Yusheng Hou, Zhe Wang, and Ruqian Wu. Two-dimensional ferromagnetic van der waals crcl 3 monolayer with enhanced anisotropy and curie temperature. *Physical Review B*, 100(22):224429, 2019.
- [48] Zhe Wang, Marco Gibertini, Dumitru Dumcenco, Takashi Taniguchi, Kenji Watanabe, Enrico Giannini, and Alberto F Morpurgo. Determining the phase diagram of atomically thin layered antiferromagnet crcl3. *Nature nanotechnology*, 14(12):1116–1122, 2019.
- [49] B Kuhlow. Magnetic ordering in crcl3 at the phase transition. *physica status solidi (a)*, 72(1):161–168, 1982.
- [50] IV Kashin, VV Mazurenko, MI Katsnelson, and AN Rudenko. Orbitally-resolved ferromagnetism of monolayer cri3. *2D Materials*, 7(2):025036, 2020.
- [51] YO Kvashnin, Anders Bergman, AI Lichtenstein, and MI Katsnelson. Relativistic exchange interactions in cr x 3 (x= cl, br, i) monolayers. *Physical Review B*, 102(11):115162, 2020.
- [52] D Soriano, AN Rudenko, MI Katsnelson, and M Rösner. Environmental screening and ligand-field effects to magnetism in cri3 monolayer. *npj Computational Materials*, 7(1):162, 2021.
- [53] Banasree Sadhukhan, Anders Bergman, Yaroslav O Kvashnin, Johan Hellsvik, and Anna Delin. Spin-lattice couplings in two-dimensional cri 3 from first-principles computations. *Physical Review B*, 105(10):104418, 2022.
- [54] Iurii Timrov, Nicola Marzari, and Matteo Cococcioni. Hp-a code for the calculation of hubbard parameters using density-functional perturbation theory. *Computer Physics Communications*, 279:108455, 2022.
- [55] Iurii Timrov, Nicola Marzari, and Matteo Cococcioni. Self-consistent hubbard parameters from density-functional perturbation theory in the ultrasoft and projector-augmented wave formulations. *Physical Review B*, 103(4):045141, 2021.
- [56] Julia Emilia Brumboiu, Soumyajyoti Haldar, Johann Luder, Olle Eriksson, Heike C Herper, Barbara Brena, and Biplab Sanyal. Ligand effects on the linear response hubbard u: the case of transition metal phthalocyanines. *The Journal of Physical Chemistry A*, 123(14):3214–3222, 2019.
- [57] Swagata Acharya, Dimitar Pashov, Brian Cunningham, Alexander N Rudenko, Malte Rösner, Myrta Grüning, Mark van Schilfgaarde, and Mikhail I Katsnelson. Electronic structure of chromium trihalides beyond density functional theory. *Physical Review B*, 104(15):155109, 2021.
- [58] Swagata Acharya, Dimitar Pashov, Alexander N Rudenko, Malte Rösner, Mark van Schilfgaarde, and Mikhail I Katsnelson. Real-and momentum-space description of the excitons in bulk and monolayer chromium tri-halides. *npj 2D Materials and Applications*, 6(1):33, 2022.
- [59] Arash A Mostofi, Jonathan R Yates, Young-Su Lee, Ivo Souza, David Vanderbilt, and Nicola Marzari. wannier90: A tool for obtaining maximally-localised wannier functions. *Computer physics communications*, 178(9):685–699, 2008.
- [60] Xu He, Nicole Helbig, Matthieu J Verstraete, and Eric Bousquet. Tb2j: A python package for computing magnetic interaction parameters. *Computer Physics Communications*, 264:107938, 2021.

- [61] Amilcar Bedoya-Pinto, Jing-Rong Ji, Avanindra K. Pandeya, Pierluigi Gargiani, Manuel Valvidares, Paolo Sessi, James M. Taylor, Florin Radu, Kai Chang, and Stuart S. P. Parkin. Intrinsic 2d-xy ferromagnetism in a van der waals monolayer. *Science*, 374(6567):616–620, 2021. doi:10.1126/science.abd5146. URL <https://www.science.org/doi/abs/10.1126/science.abd5146>.
- [62] Zhaowei Zhang, Jingzhi Shang, Chongyun Jiang, Abdullah Rasmita, Weibo Gao, and Ting Yu. Direct photoluminescence probing of ferromagnetism in monolayer two-dimensional crbr₃. *Nano letters*, 19(5):3138–3142, 2019.
- [63] Wei-Bing Zhang, Qian Qu, Peng Zhu, and Chi-Hang Lam. Robust intrinsic ferromagnetism and half semiconductivity in stable two-dimensional single-layer chromium trihalides. *Journal of Materials Chemistry C*, 3(48):12457–12468, 2015.
- [64] Lucas Webster and Jia-An Yan. Strain-tunable magnetic anisotropy in monolayer crcl₃, crbr₃, and cri₃. *Physical Review B*, 98(14):144411, 2018.
- [65] Tommaso Gorni, Oscar Baseggio, Pietro Delugas, Iurii Timrov, and Stefano Baroni. First-principles study of the gap in the spin excitation spectrum of the cri₃ honeycomb ferromagnet. *arXiv preprint arXiv:2212.09516*, 2022.
- [66] Liqin Ke and Mikhail I Katsnelson. Electron correlation effects on exchange interactions and spin excitations in 2d van der waals materials. *npj Computational Materials*, 7(1):4, 2021.
- [67] Pietro Delugas, Oscar Baseggio, Iurii Timrov, Stefano Baroni, and Tommaso Gorni. Magnon-phonon interactions open a gap at the dirac point in the spin-wave spectra of cri₃ 2d magnets. *arXiv preprint arXiv:2105.04531*, 2021.
- [68] Raí M Menezes, Denis Šabani, Cihan Bacaksiz, Clécio C de Souza Silva, and Milorad V Milošević. Tailoring high-frequency magnonics in monolayer chromium trihalides. *2D Materials*, 9(2):025021, 2022.
- [69] Ahmet Avsar, Jun You Tan, T Taychatanapat, J Balakrishnan, GKW Koon, Y Yeo, J Lahiri, A Carvalho, AS Rodin, ECT O’Farrell, et al. Spin-orbit proximity effect in graphene. *Nature communications*, 5(1):4875, 2014.
- [70] Martin Gmitra and Jaroslav Fabian. Graphene on transition-metal dichalcogenides: A platform for proximity spin-orbit physics and optospintronics. *Physical Review B*, 92(15):155403, 2015.
- [71] Kyung-Hwan Jin and Seung-Hoon Jhi. Proximity-induced giant spin-orbit interaction in epitaxial graphene on a topological insulator. *Physical Review B*, 87(7):075442, 2013.
- [72] Paolo Giannozzi, Stefano Baroni, Nicola Bonini, Matteo Calandra, Roberto Car, Carlo Cavazzoni, Davide Ceresoli, Guido L Chiarotti, Matteo Cococcioni, Ismaila Dabo, et al. Quantum espresso: a modular and open-source software project for quantum simulations of materials. *Journal of physics: Condensed matter*, 21(39):395502, 2009.
- [73] Matthias Ernzerhof and Gustavo E Scuseria. Assessment of the perdew–burke–ernzerhof exchange-correlation functional. *The Journal of chemical physics*, 110(11):5029–5036, 1999.
- [74] John D Head and Michael C Zerner. A broyden–fletcher–goldfarb–shanno optimization procedure for molecular geometries. *Chemical physics letters*, 122(3):264–270, 1985.
- [75] Hendrik J Monkhorst and James D Pack. Special points for brillouin-zone integrations. *Physical review B*, 13(12):5188, 1976.
- [76] Joren Vanherck, Cihan Bacaksiz, Bart Sorée, Milorad V Milošević, and Wim Magnus. 2d ferromagnetism at finite temperatures under quantum scrutiny. *Applied Physics Letters*, 117(5):052401, 2020.
- [77] S Toth and B Lake. Linear spin wave theory for single-q incommensurate magnetic structures. *Journal of Physics: Condensed Matter*, 27(16):166002, 2015.
- [78] JHP Colpa. Diagonalization of the quadratic boson hamiltonian. *Physica A: Statistical Mechanics and its Applications*, 93(3-4):327–353, 1978.

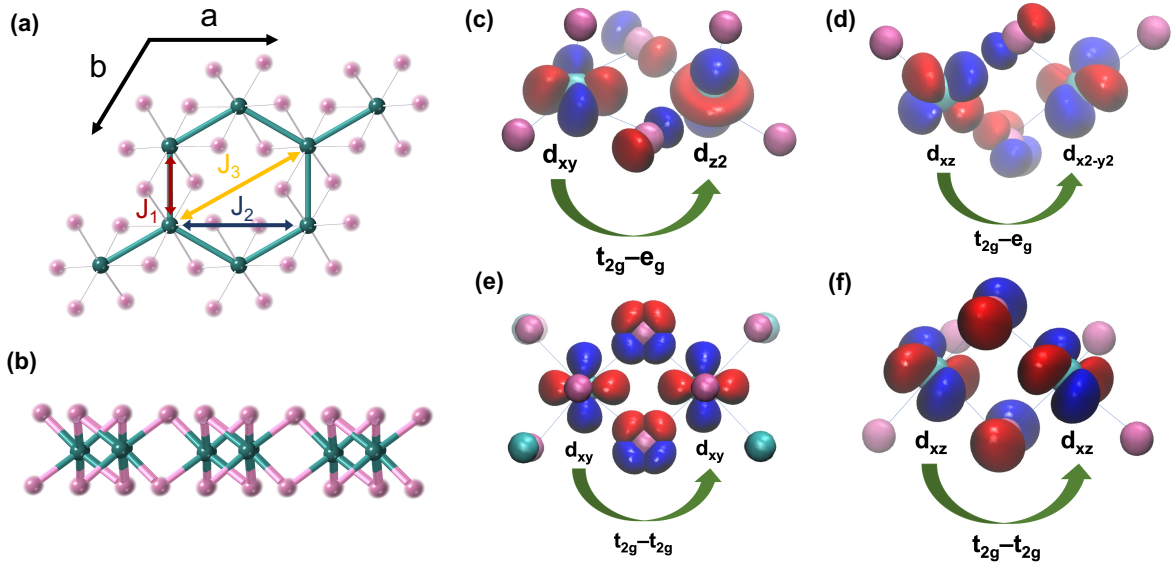


FIG. 1. (a) Top view of a CrX₃ monolayer indicating the main exchange interactions. (b) Side view of the same structure. (c-f) Calculated maximally localized Wannier functions representing the atomic orbitals responsible of J₁ interaction in CrX₃. (c,d) t_{2g}-e_g (FM) and (e,f) t_{2g}-t_{2g} (AFM) pathways.

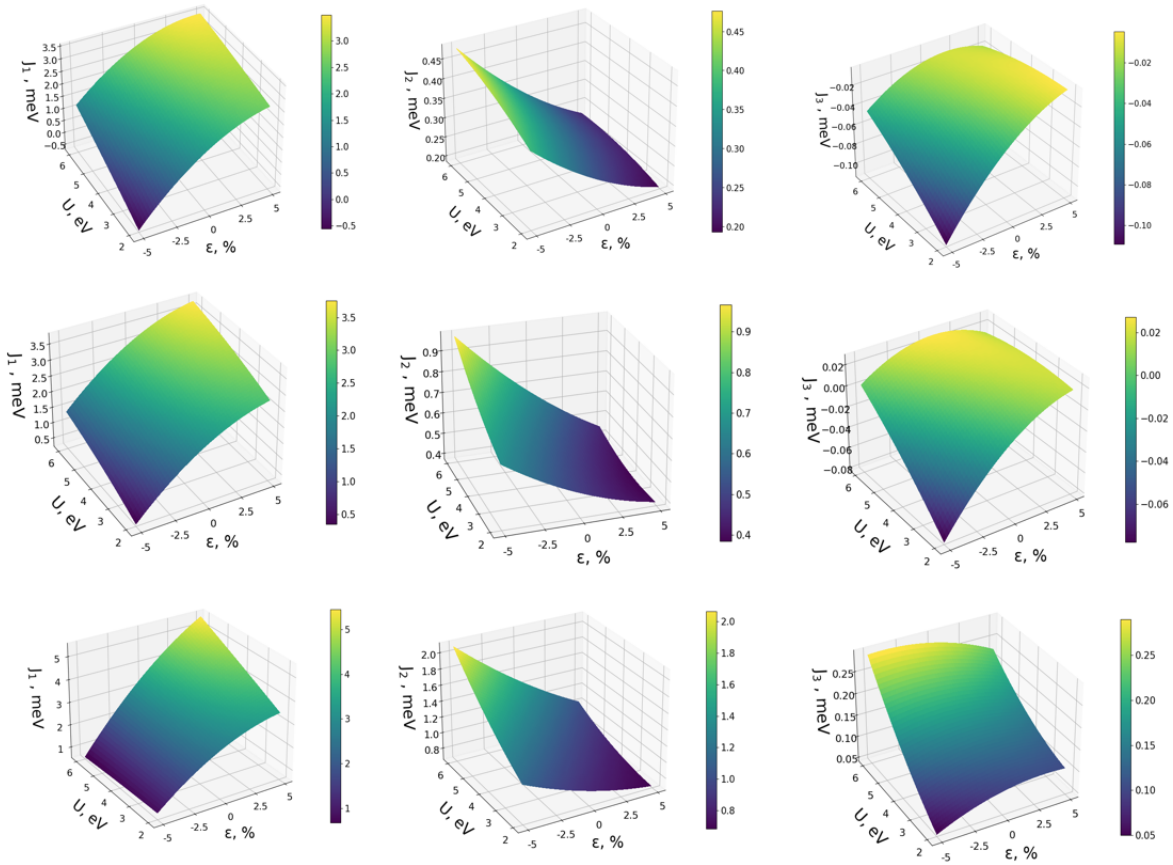


FIG. 2. High-density 3D surface plots of isotropic exchange interactions as a function of biaxial strain and Hubbard U in CrCl₃ (top), CrBr₃ (center) and CrI₃ (bottom).

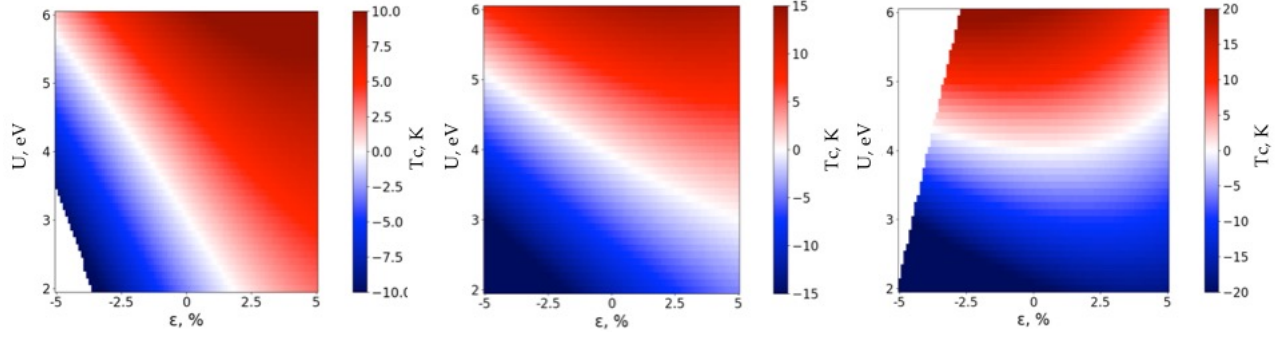


FIG. 3. Evolution of Curie temperature under biaxial strain and Hubbard U for (left) CrCl_3 , (center) CrBr_3 and (right) CrI_3 .

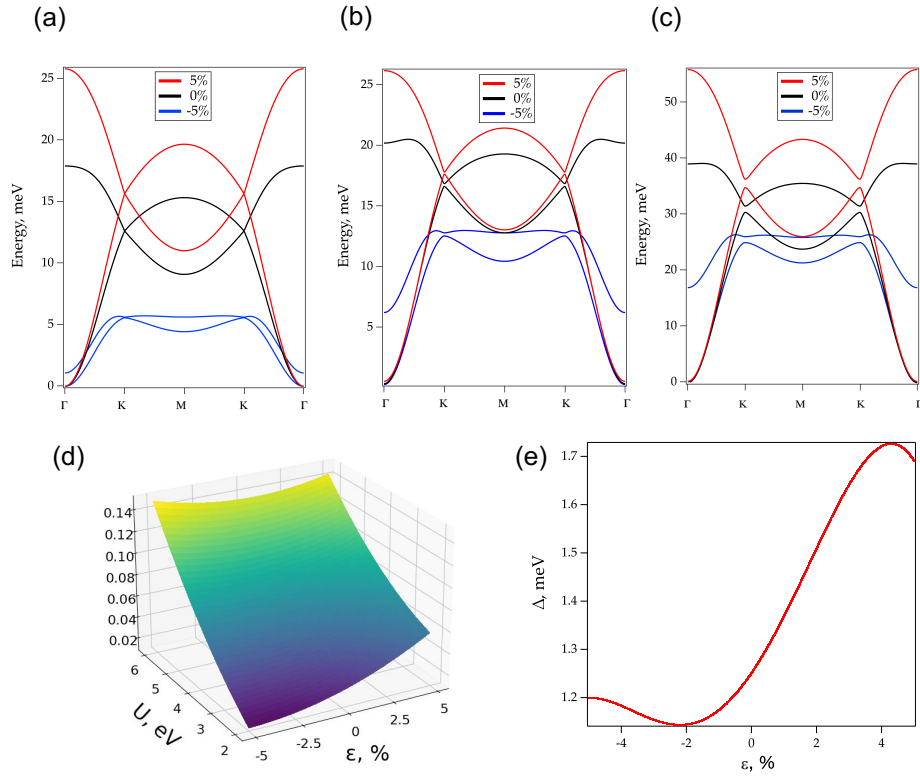


FIG. 4. Magnon dispersion of (a) CrCl_3 , (b) CrBr_3 and (c) CrI_3 , black indicates 0% strain, and red (blue) 5 (-5)%. (d) Effective equation representing the z component of the 2nd neighbour DM interaction in CrI_3 . (e) Evolution of the Δ_k gap in CrI_3 .